

The suppression of Curie temperature by Sr doping in diluted ferromagnetic semiconductor $(\text{La}_{1-x}\text{Sr}_x)(\text{Zn}_{1-y}\text{Mn}_y)\text{AsO}$

CUI DING¹, XIN GONG¹, HUIYUAN MAN¹, GUOXIANG ZHI¹, SHENGLI GUO¹, YANG ZHAO^{2,3}, HANGDONG WANG⁴, BIN CHEN⁴ AND F.L. NING¹ ^(a)

¹ Department of Physics, Zhejiang University - Hangzhou 310027, China

² NIST center for Neutron Research, National Institute of Standards and Technology, Gaithersburg, Maryland 20899, USA

³ Department of Materials Science and Engineering, University of Maryland, College Park, Maryland 20742, USA

⁴ Department of Physics, Hangzhou Normal University - Hangzhou 310016, China

PACS 75.50.Pp – Magnetic semiconductors

PACS 75.47.Lx – Magnetic Oxides

PACS 75.30.Cr – Saturation moments and magnetic susceptibilities

Abstract – $(\text{La}_{1-x}\text{Sr}_x)(\text{Zn}_{1-y}\text{Mn}_y)\text{AsO}$ is a two dimensional diluted ferromagnetic semiconductor that has the advantage of decoupled charge and spin doping. The substitution of Sr^{2+} for La^{3+} and Mn^{2+} for Zn^{2+} into the parent semiconductor LaZnAsO introduces hole carriers and spins, respectively. This advantage enables us to investigate the influence of carrier doping on the ferromagnetic ordered state through the control of Sr concentrations in $(\text{La}_{1-x}\text{Sr}_x)(\text{Zn}_{0.9}\text{Mn}_{0.1})\text{AsO}$. 10 % Sr doping results in a ferromagnetic ordering below $T_C \sim 30$ K. Increasing Sr concentration up to 30 % heavily suppresses the Curie temperature and saturation moments. Neutron scattering measurements indicate that no structural transition occurs for $(\text{La}_{0.9}\text{Sr}_{0.1})(\text{Zn}_{0.9}\text{Mn}_{0.1})\text{AsO}$ below 300 K.

Introduction. – The observation of ferromagnetic ordering in III-V $(\text{Ga},\text{Mn})\text{As}$ below Curie temperature $T_C \sim 60$ K by Ohno et al [1] has generated extensive research into the diluted ferromagnetic semiconductors (DFS). After almost two decades of efforts, T_C has been improved to as high as 200 K with Mn doping level of ~ 12 % [2–5]. This temperature is still far below room temperature which is the prerequisite for practical application of spintronics [6]. Improving T_C in homogenous $(\text{Ga},\text{Mn})\text{As}$ thin films is one of the objectives in the research of DFS. On the other hand, understanding the mechanism of ferromagnetic ordering is hindered by some inherent difficulties. In $(\text{Ga},\text{Mn})\text{As}$, the substitution of Mn^{2+} for Ga^{3+} provides not only local moments but also hole carriers. It is generally believed that ferromagnetic ordering can arise only when spins are effectively mediated by carriers [7]. However, during the fabrication of $(\text{Ga},\text{Mn})\text{As}$ thin films, some Mn atoms enter interstitial sites and behave as a double doner, which make it difficult to determine precisely the amount of Mn that substitute Ga at

ionic sites. Seeking for new ferromagnetic semiconductor systems with more controllable charge and spin densities might be helpful to understand the general mechanism of ferromagnetism in DFS.

Recently, several bulk DFS systems that are derivatives of Fe-based high temperature superconductor have been reported. The first Fe-based superconductor is 1111-type oxypnictides, $\text{LaFeAs}(\text{O}_{1-x}\text{F}_x)$ [8], which has a superconducting transition temperature $T_c = 26$ K. With identical two dimensional crystal structure, three 1111 type DFS systems, $(\text{La},\text{Ba})(\text{Zn},\text{Mn})\text{AsO}$ with $T_C \sim 40$ K [9], $(\text{La},\text{Ca})(\text{Zn},\text{Mn})\text{SbO}$ with $T_C \sim 40$ K [10], $(\text{La},\text{Sr})(\text{Cu},\text{Mn})\text{SO}$ [11] with $T_C \sim 210$ K have been reported. Similarly, two bulk form DFS systems, $(\text{Ba},\text{K})(\text{Zn},\text{Mn})_2\text{As}_2$ [12] with $T_C \sim 180$ K and $(\text{Ba},\text{K})(\text{Cd},\text{Mn})_2\text{As}_2$ with $T_C \sim 17$ K [13], have been reported. These two systems are structurally identical to that of 122 type iron pnictides superconductor, $(\text{Ba},\text{K})\text{Fe}_2\text{As}_2$ ($T_c = 38$ K) [14]. The third DFS family reported recently is $\text{Li}(\text{Zn},\text{Mn})\text{Pn}$ ($\text{Pn} = \text{P}, \text{As}$) [15, 16] with $T_C \sim 50$ K, which are fabricated by doping Mn into the I-II-V direct gap semiconductors LiZnPn ($\text{Pn} = \text{P},$

^(a)Electronic address: ningfl@zju.edu.cn

As). LiZnAs can also be viewed as a derivative of the third family of Fe-based superconductors LiFeAs ($T_c = 18$ K) [17]. The fourth family of Fe-based superconductors is 11 type FeSe $_{1+\delta}$ ($T_c = 8$ K) [18], which can be paralleled to the well investigated II-VI DFS, i.e., (Zn,Mn)Se. There are two more families of Fe-based superconductors, namely, 32522 type (Ca $_3$ Al $_2$ O $_5$)Fe $_2$ As $_2$ ($T_c \sim 30.2$ K) [19] and 42622 type Sr $_4$ V $_2$ O $_6$ Fe $_2$ As $_2$ ($T_c \sim 37.2$ K) [20]. Very recently, 32522 type DFS Sr $_3$ La $_2$ O $_5$ (Zn,Mn) $_2$ As $_2$ with Curie temperature $T_C \sim 40$ K [21] and 42622 type DFS Sr $_4$ Ti $_2$ O $_6$ (Zn,Mn) $_2$ As $_2$ with $T_C \sim 25$ K have been reported [22].

Different to thin film form (Ga,Mn)As specimens, above new DFS systems are all in bulk form. The availability of a specimen in bulk form enables the investigation of DFS by powerful magnetic probes including NMR (Nuclear Magnetic Resonance), μ SR (muon Spin Rotation) and neutron scattering. NMR investigation of I-II-V DFS Li(Zn,Mn)P by Ding *et al.* has shown that the spin-lattice relaxation rate $\frac{1}{T_1}$ of Li(0) site (zero means that no Mn atoms at N.N. (nearest neighbor) Zn site of Li) exhibits a kink around T_C , which indicates that Li(0) sites are indeed under the influence of ferromagnetic Mn spin fluctuations [23]. Furthermore, $\frac{1}{T_1}$ of Li(Mn) site is temperature independent above T_C , i.e., $\frac{1}{T_1} \sim 400$ s $^{-1}$, indicating that Mn spin-spin interaction extends over many unit cells with an interaction energy scale $|J| \sim 100$ K. On the other hand, μ SR measurements have shown that bulk form I-II-V, 1111 and 122 DFSs all share a common ferromagnetic mechanism as that of (Ga,Mn)As thin film [9, 12, 15].

Another important feature of the newly fabricated bulk DFSs is that they all have advantages of decoupled carriers and spins doping. Here Mn $^{2+}$ substitution for Zn $^{2+}$ introduces only spins, and carriers are introduced at a different site. Only when both carriers and spins are introduced simultaneously, can ferromagnetic ordering develop [9]. In this paper, we dope Sr and Mn into the direct gap parent semiconductor LaZnAsO up to the doping level of 30 %. We found that chemical solubility is 20 %, which is much higher than 10% of doping Ba. This allows us to investigate the high doping regime in a more reliable manner. The Curie temperature T_C in (La $_{1-x}$ Sr $_x$)(Zn $_{1-y}$ Mn $_y$)AsO increases from 30 K of $x = 0.10$ to 35 K of $x = 0.20$, but decreases to 27 K for $x = 0.30$. For a fixed Mn concentration of $x = 0.10$, we found that more hole doping than 10 % suppresses both T_C and the saturation moments. 30 % hole doping suppresses saturation moment by almost an order, and no strong enhancement in magnetization curve that corresponds to the ferromagnetic ordering has been observed.

Experiments. – Polycrystalline specimens of (La $_{1-x}$ Sr $_x$)(Zn $_{1-y}$ Mn $_y$)AsO were prepared through solid state reaction method by mixing intermediate products LaAs, ZnAs, MnAs, ZnO, MnO and SrO with nominal concentrations. The mixture was then made into pellets and heated to 1150 °C slowly. It was kept at 1150 °C for

40 hours before cooling down with shutting off furnace. The intermediate products LaAs, ZnAs and MnAs were prior produced with mixing high purity elements La, Zn, Mn and As and heating at 900 °C for 10 hour. The processes of mixing were carried in high purity Ar atmosphere in a glove box and the mixtures were sealed in an evacuated silica tube before heating. The polycrystals were characterized by X-ray powder diffraction and dc magnetization by SQUID (Superconducting Quantum Interference Device). The electrical resistance was measured on sintered pellets with typical four-probe method. Neutron scattering measurements were performed at NIST Center for Neutron Research (NCNR) using BT-1 powder Diffractometer.

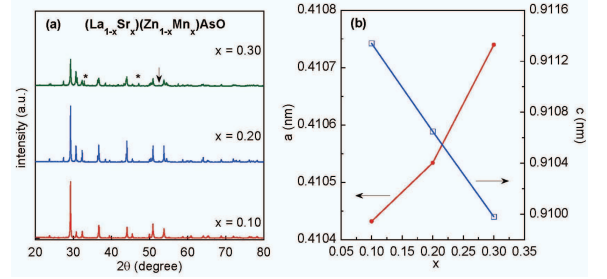


Fig. 1: (Color online) (a) Powder X-ray diffraction pattern of (La $_{1-x}$ Sr $_x$)(Zn $_{1-y}$ Mn $_y$)AsO ($x = y = 0.10, 0.20, 0.30$). Traces of La $_2$ O $_3$ (\downarrow) and ZnAs $_2$ ($*$) impurities are marked for $x = 0.30$. (b) Lattice parameters for a axis (red solid circles) and c axis (blue open squares).

Results and discussion. – In Fig. 1(a), we show the powder X-ray diffraction patterns of (La $_{1-x}$ Sr $_x$)(Zn $_{1-y}$ Mn $_y$)AsO with Sr and Mn of equal doping levels ($x = y = 0.10, 0.20, 0.30$). As demonstrated by the Reitveld refinement for LaZnAsO compound [9], the Bragg peaks of the specimens can be well indexed into a tetragonal crystal structure of space group P4/nmm. The lattice parameters for three concentrations are shown in figure 1(b). The lattice constant a monotonically increases while c monotonically decreases with Sr and Mn doping, indicating successful solid solution of (La,Sr) and (Zn,Mn). We find the chemical solubility is as high as 20 %, much higher than the case of Ba and Mn doping into LaZnAsO which is only 10 % [9]. This can be attributed to the much closer atomic radius of La $^{3+}$ (0.106 nm) and Sr $^{2+}$ (0.113 nm). Traces of La $_2$ O $_3$ (\downarrow) and ZnAs $_2$ ($*$) impurities are observed for $x = 0.30$ concentration. These impurities are non-magnetic, which do not affect our discussion below.

We show results of electrical resistance measured for parent compound LaZnAsO, 10 % Sr doped specimen (La $_{0.9}$ Sr $_{0.1}$)ZnAsO, and 10 % Sr and Mn doped specimen (La $_{0.9}$ Sr $_{0.1}$)(Zn $_{0.9}$ Mn $_{0.1}$)AsO in Fig. 2. The par-

ent compound is a direct-gap semiconductor with a band gap of ~ 1.5 eV [24], and it displays a typical semiconducting behavior. 10 % Sr substitution for La readily changes the semiconductor into a metal, as demonstrated by the decreasing resistivity with temperature decreasing. More interestingly, once 10 % Mn are doped into $(\text{La}_{0.9}\text{Sr}_{0.1})\text{ZnAsO}$, the specimen returns to a semiconducting behavior. It seems that spins induced by Mn atoms localize the hole carriers. We do a tentative fitting of the $\rho(T)$ data for $(\text{La}_{0.9}\text{Sr}_{0.1})(\text{Zn}_{0.9}\text{Mn}_{0.1})\text{AsO}$ near room temperature with a thermally activated conductivity, $\frac{1}{\rho} = C \exp(-E_a/2k_B T)$. The fitting is good, and the scenario of the disorder induced localization mechanism seems not applicable here. We also find an activation energy of 0.056 eV, which is much smaller than the gap energy of LaZnAsO .

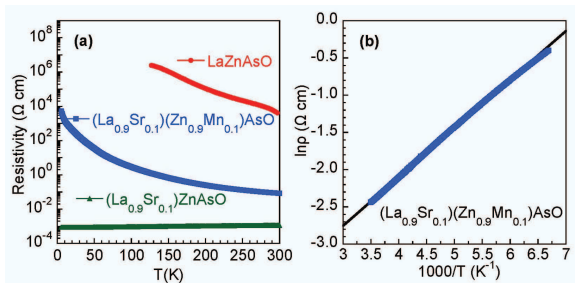


Fig. 2: (Color online) (a) The electrical resistivity for parent compound LaZnAsO , 10 % Sr doped specimen $(\text{La}_{0.9}\text{Sr}_{0.1})\text{ZnAsO}$, and 10 % Sr and Mn doped specimen $(\text{La}_{0.9}\text{Sr}_{0.1})(\text{Zn}_{0.9}\text{Mn}_{0.1})\text{AsO}$. (b) The fitting of resistivity for $(\text{La}_{0.9}\text{Sr}_{0.1})(\text{Zn}_{0.9}\text{Mn}_{0.1})\text{AsO}$ with an activation function.

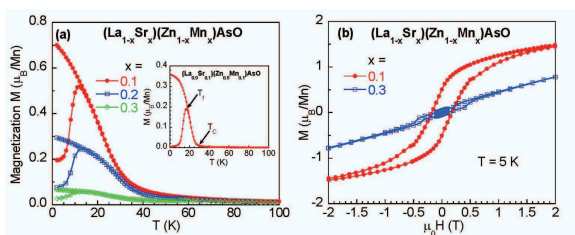


Fig. 3: (Color online) (a) dc magnetization M measured under ZFC and FC condition for $(\text{La}_{1-x}\text{Sr}_x)(\text{Zn}_{1-y}\text{Mn}_y)\text{AsO}$ ($x = y = 0.10, 0.20, 0.30$) at $\mu_0 H = 0.1$ Tesla; the inset shows M of $(\text{La}_{0.9}\text{Sr}_{0.1})(\text{Zn}_{0.9}\text{Mn}_{0.1})\text{AsO}$ measured at $\mu_0 H = 0.005$ Tesla, T_C and T_f are marked by arrows. (b) The isothermal magnetization measurements for $(\text{La}_{1-x}\text{Sr}_x)(\text{Zn}_{1-y}\text{Mn}_y)\text{AsO}$ ($x = y = 0.10, 0.30$) at 5 K.

In Fig. 3(a), we show dc magnetization curve of $(\text{La}_{1-x}\text{Sr}_x)(\text{Zn}_{1-y}\text{Mn}_y)\text{AsO}$ ($x = y = 0.10, 0.20, 0.30$) measured with 0.1 Tesla external field under zero-field-cooled (ZFC) and field-cooled (FC) condition (note that Sr atoms and Mn are in the same doping level). We define the Curie temperature of ferromagnetic ordering, T_C , as the temperature where magnetization curve measured at 0.005 Tesla displays a sharp enhancement, as marked by

the arrow in the inset of Fig. 3(a). As the doping level increases, T_C increases from 30 K for $x = 0.10$ to 35 K for $x = 0.20$, and then decreases to 27 K for $x = 0.30$. The saturation moment is $0.71 \mu_B/\text{Mn}$ for $x = 0.10$, which is comparable to that of $(\text{La}_{0.9}\text{Ba}_{0.1})(\text{Zn}_{0.9}\text{Mn}_{0.1})\text{AsO}$ [9]. The saturation moment is suppressed monotonically to $0.07 \mu_B/\text{Mn}$ at the doping level of $x = 0.30$. Another feature of magnetization curve is that ZFC and FC curves split at a temperature below T_C , as marked by the arrow in inset of Fig. 3(a). This temperature is defined as T_f , which is the onset temperature of static spin freezing, as has been investigated by μSR measurement of $(\text{La}, \text{Ba})(\text{Zn}, \text{Mn})\text{AsO}$ [9]. T_f decreases monotonically from 17 K ($x = 0.10$) to 12 K ($x = 0.30$).

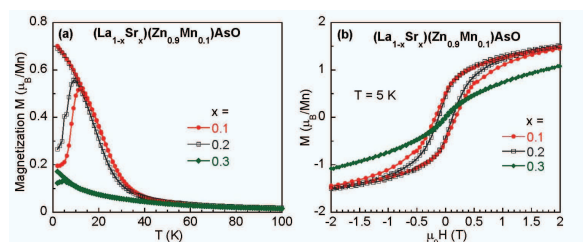


Fig. 4: (Color online) (a) dc magnetization M measured under ZFC and FC condition for $(\text{La}_{1-x}\text{Sr}_x)(\text{Zn}_{0.9}\text{Mn}_{0.1})\text{AsO}$ ($x = 0.10, 0.20, 0.30$) at $\mu_0 H = 0.1$ Tesla. (b) The isothermal magnetization measurements for $(\text{La}_{1-x}\text{Sr}_x)(\text{Zn}_{0.9}\text{Mn}_{0.1})\text{AsO}$ ($x = 0.10, 0.20, 0.30$) at 5 K.

The isothermal magnetization at 5 K for $(\text{La}_{0.9}\text{Sr}_{0.1})(\text{Zn}_{0.9}\text{Mn}_{0.1})\text{AsO}$ and $(\text{La}_{0.7}\text{Sr}_{0.3})(\text{Zn}_{0.7}\text{Mn}_{0.3})\text{AsO}$ is shown in figure 3(b). With the increasing of Sr and Mn concentrations, the coercive fields are quickly suppressed from 0.178 Tesla to 0.102 Tesla. For comparison, the coercive field of $(\text{Ga}_{0.965}\text{Mn}_{0.035})\text{As}$ is ~ 0.005 Tesla [1]. On the other hand, the saturation remanence of $(\text{La}_{0.9}\text{Sr}_{0.1})(\text{Zn}_{0.9}\text{Mn}_{0.1})\text{AsO}$ is $\sim 0.5 \mu_B/\text{Mn}$, an order of magnitude larger than $\sim 0.04 \mu_B/\text{Mn}$ of $(\text{La}_{0.7}\text{Sr}_{0.3})(\text{Zn}_{0.7}\text{Mn}_{0.3})\text{AsO}$. The suppression of T_C , saturation moments, and coercive fields with higher Mn doping levels is very likely arising from competition of direct antiferromagnetic exchange interaction from N.N. Mn atoms at Zn sites. The probability to find two Mn at N.N. Zn sites is $P(N; x) = C_N^2 x^2 (1-x)^{4-N} = 29.16\%$ for $x = 0.10$ (where $N = 4$ and $x = 0.10$). This probability increases to 41.16 % for the doping level of $x = 0.30$. The direct antiferromagnetic coupling between Mn-Mn pairs eventually results in the antiferromagnetic ordering in LaMnAsO at $T_N = 317$ K [25].

Since we can control spins and carriers separately, it will be interesting to investigate the influence of different carrier doping levels on the magnetic state at a fixed Mn concentration. We fix Mn at the level of 0.10, and enhance the doping levels of Sr up to 20 % and 30 %. The ZFC and FC dc-magnetization curves of three specimens are plotted in Fig. 4(a) and their isothermal magnetiza-

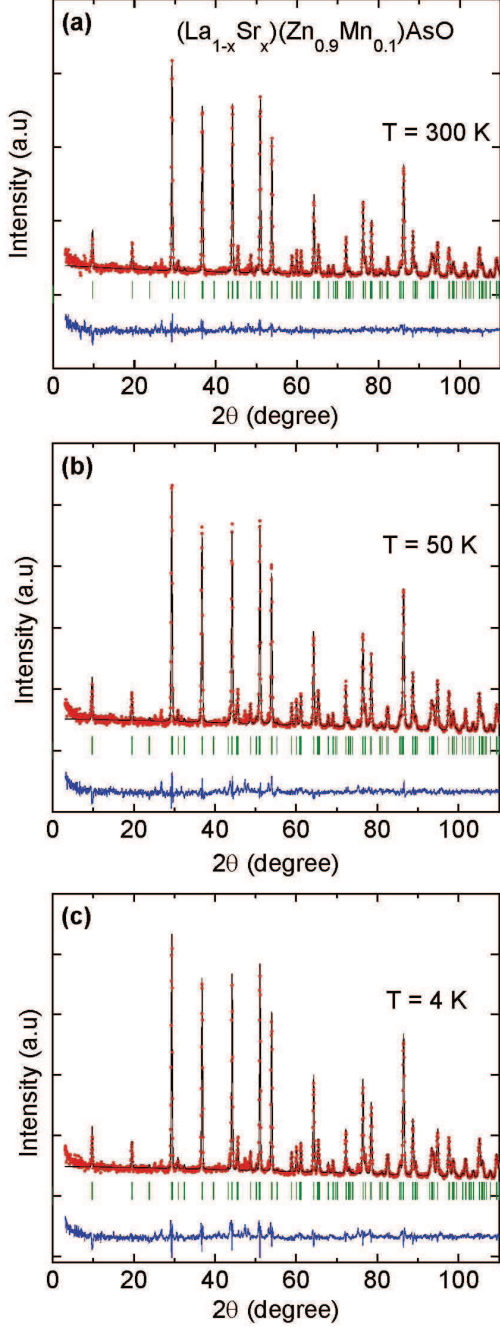


Fig. 5: Neutron diffraction pattern for the powder specimen of $(\text{La}_{0.9}\text{Sr}_{0.1})(\text{Zn}_{0.9}\text{Mn}_{0.1})\text{AsO}$ at 300K (a), 50K (b) and 4K(c) at NIST. Error bars are smaller than plot symbols.

tion at 5 K are plotted in Fig. 4(b). Compared to 10 % Sr doping sample, both T_C and saturation moments are only slightly suppressed with 20 % Sr doping. When Sr doping level is increased to $x = 0.30$, both T_C and saturation moments are heavily suppressed. The saturation moment decreases from $0.71 \mu_B/\text{Mn}$ for $x = 0.10$ to $0.17 \mu_B/\text{Mn}$ for $x = 0.30$. Similarly, T_f decreases from 17 K to 5 K and coercive field declines from 0.178 Tesla to 0.022 Tesla. The saturation remanence decreases from

$\sim 0.5 \mu_B/\text{Mn}$ for $x = 0.10$ to $0.03 \mu_B/\text{Mn}$ for $x = 0.30$. In early stage of DFS research, it has been theoretically proposed that spins are mediated by hole carriers through RKKY interaction [7]. We can write the RKKY exchange interaction as $J \sim \frac{\cos(2k_F r)}{r^3}$, where k_F is the radius of Fermi surface if assuming the Fermi surface is a spherical shape, and r the distance between two localized moments. The first oscillation period of RKKY interaction supports ferromagnetic coupling. In present work, doping more Sr into $(\text{La}_{1-x}\text{Sr}_x)(\text{Zn}_{0.9}\text{Mn}_{0.1})\text{AsO}$ has introduced extra hole carriers, which modifies the density of states and the Fermi surface, and subsequently the ferromagnetic ordering.

To investigate the spin structure, we conducted neutron diffraction of the powder specimen $(\text{La}_{0.9}\text{Sr}_{0.1})(\text{Zn}_{0.9}\text{Mn}_{0.1})\text{AsO}$ (which has the largest saturation moment size) at 4 K, 50 K and 300 K at NCNR, and show the results in Fig. 5. We found that neutron powder diffraction pattern is in line with X-rays diffraction pattern, and no impurities are observed. This indicates that Mn atoms are indeed substituted into Zn sites. We spent 8 hours for a 3 grams sample at 4 K, but still could not separate the magnetic diffraction peaks from the structural ones. In $(\text{La}_{0.9}\text{Sr}_{0.1})(\text{Zn}_{0.9}\text{Mn}_{0.1})\text{AsO}$, the average moment size is only $\sim 0.07 \mu_B/\text{Mn}(\text{Zn})$, which is smaller than the limit of neutron resolution $\sim 0.1 \mu_B$ with current experiment configuration. None the less, we do not observe structural phase transition from 300 K to 4 K, which cross $T_C = 30$ K.

Summary and Conclusion. – To summarize, we successfully synthesized a new DFS system $(\text{La}_{1-x}\text{Sr}_x)(\text{Zn}_{1-x}\text{Mn}_x)\text{AsO}$ with doping level up to 30 %. Maximum T_C is as high as 35 K at the doping of $x = 0.20$. With the advantage of decoupled spin and carrier doping, we could investigate the influence of carrier concentration on the ferromagnetic ordering. We found that 30 % Sr substitution for La in $(\text{La}_{1-x}\text{Sr}_x)(\text{Zn}_{0.9}\text{Mn}_{0.1})\text{AsO}$ suppresses the ferromagnetic ordering, leaving a spin glass like magnetic ordered state. As we have shown in $(\text{LaBa})(\text{ZnMn})\text{AsO}$ [9], spins can not order ferromagnetically without carrier doping. Our experimental evidence shown in this work unequivocally demonstrates that too much carriers suppresses both the Curie temperature and the saturation moments. In other words, too much carriers are detrimental to the ferromagnetic ordering as well. It requires a delicate balance between carriers and spins to achieve highest T_C . In addition, our neutron scattering experiments rule out the possibility of a structural transition between 300 K and 4 K for $(\text{La}_{0.9}\text{Sr}_{0.1})(\text{Zn}_{0.9}\text{Mn}_{0.1})\text{AsO}$ specimen. Finally, as stated previously, the common two dimensional crystal structure shared by ferromagnetic $(\text{La}_{1-x}\text{Sr}_x)(\text{Zn}_{1-y}\text{Mn}_y)\text{AsO}$, 1111-type Fe-based high temperature superconductors and antiferromagnetic LaMnAsO , makes it possible to make various junctions through As layers.

The work at Zhejiang was supported by National Basic Research Program of China (No.2014CB921203, 2011CBA00103), NSF of China (No. 11274268). F.L. Ning acknowledges helpful discussions with I. Mazin, I. Zutic, Y.J. Uemura and C.Q. Jin.

REFERENCES

- [1] OHNO H., SHEN A., MATSUKURA F., OIWA A., ENDO A., KATSUMOTO S., AND IYE Y., *Appl. Phys. Lett.*, **69** (1996) 363.
- [2] WANG M., CAMPION R. P., RUSHFORTH A. W., EDMONDS K. W., FOXON C. T., AND GALLAGHER B. L., *Appl. Phys. Lett.*, **93** (2008) 132103.
- [3] CHEN L., YAN S., XU P. F., WANG W. Z., DENG J. J., QIAN X., JI Y. AND ZHAO J. H., *Appl. Phys. Lett.*, **95** (2009) 182505.
- [4] CHEN L., YANG X., YANG F. H., MISURACA J., XIONG P., MOLNAR S. V. AND ZHAO J. H., *Nano. Lett.*, **11** (2011) 2584.
- [5] DIETL T. AND OHNO H., *Rev. Mod. Phys.*, **86** (2014) 187.
- [6] ZUTIC I., FABIAN J. AND DAS SARMA S., *Rev. Mod. Phys.*, **76** (2004) 323.
- [7] DIETL T., OHNO H., MATSUKURA F., CIBERT J. AND FERRAND D., *Science*, **287** (2000) 1019.
- [8] KAMIHARA Y., WATANABE T., HIRANO M. AND HOSONO H., *J. Am. Chem. Soc.*, **130** (2008) 3296.
- [9] DING C., MAN H. Y., QIN C., LU J. C., SUN Y. L., WANG Q., YU B. Q., FENG C. M., GOKO T., ARGUELLO C. J., LIU L., FRANDSEN B. A., UEMURA Y. J., WANG H. D., LUETKENS H., MORENZONI E., HAN W., JIN C. Q., MUNSIE T., WILLIAMS T. J., DORTENZIO R. M., MEDINA T., LUKE G. M., IMAI T. AND NING F. L., *Phys. Rev. B*, **88** (2013) 041102(R).
- [10] HAN W., ZHAO K., WANG X. C., LIU Q. Q., NING F. L., DENG Z., LIU Y., DING C. AND JIN C. Q., *Sci. China Phys. Mech. Astron.*, **56** (2013) 2026.
- [11] YANG X. J., LI Y. K., SHEN C. Y, SI B. Q, SUN Y. L., TAO Q., CAO C., XU Z. A., AND ZHANG F. C., *Appl. Phys. Lett.*, **103** (2013) 022410.
- [12] ZHAO K., DENG Z., WANG X. C., HAN W., ZHU J. L., LI X., LIU Q. Q., YU R. C., GOKO T., FRANDSEN B., LIU L., NING F. L., UEMURA Y. J., DABKOWSKA H., LUKE G. M., LUETKENS H., MORENZONI E., DUNSIGER S. R., SENYSHYN A., BONI P. AND JIN C. Q., *Nat. Commun.*, **4** (2013) 1442.
- [13] YANG X. J., LI Y. K., ZHANG P., LUO Y. K., CHEN Q., FENG C. M., CAO C., DAI J. H., TAO Q., CAO G. H. AND XU Z. A., *J. Appl. Phys.*, **114** (2013) 223905.
- [14] ROTTER M., TEGEL M. AND JOHRENDT D., *Phys. Rev. Lett.*, **101** (2008) 107006.
- [15] DENG Z., JIN C.Q., LIU Q.Q., WANG X.C., ZHU J.L., FENG S.M., CHEN L.C., YU R.C., ARGUELLO C., GOKO T., NING F.L., ZHANG J.S., WANG Y.Y., ACZEL A.A., MUNSIE T., WILLIAMS T.J., LUKE G.M., KAKESHITA T., UCHIDA S., HIGEMOTO W., ITO T.U., GU B., MAEKAWA S., MORRIS G.D., AND UEMURA Y.J., *Nature Communications*, **2** (2011) 422.
- [16] DENG Z., ZHAO K., GU B., HAN W., ZHU J.L., WANG X.C., LI X., LIU Q.Q., YU R.C., GOKO T., FRANDSEN B., LIU L., ZHANG J.S., WANG Y.Y., NING F.L., MAEKAWA S., UEMURA Y.J., AND JIN C.Q., *Phys. Rev. B*, **88** (2013) 081203(R).
- [17] WANG X. C., LIU Q. Q., LV Y. X., GAO W. B., YANG, L. X., YU R. C., LI F. Y. AND JIN C. Q., *Solid State Commun.*, **148** (2008) 538.
- [18] HSU F. C., LUO J. Y., YEH K. W., CHEN T. K., HUANG T.W., WU P. M., LEE Y. C., HUANG Y. L., CHU Y. Y., YAN D. C. AND WU M. K., (2008) PROC. NATL. ACAD. SCI. U.S.A., **105**, 14262.
- [19] SHIRAGE P. M., KIHOU K., LEE C. H., KITO H., EISAKI H. AND IYO A., *J. Am. Chem. Soc.*, **133** (2011) 9630.
- [20] ZHU X. Y., HAN F., MU G., CHENG P., SHEN B., ZENG B. AND WEN H. H., *Phys. Rev. B*, **79** (2009) 220512(R).
- [21] MAN H. Y., QIN C., DING C., WANG Q., GONG X., GUO S. L., WANG H. D., CHEN B. AND NING F. L., *EPL*, **105** (2014) 67004.
- [22] WANG Q., NING F.L. ET.AL. TO BE SUBMITTED.,
- [23] DING C., QIN C., MAN H. Y., IMAI T., AND NING F. L., *Phys. Rev. B*, **88** (2013) 041108(R).
- [24] KAYANUMA K., KAWAMURA R., HIRAMATSU H. ET AL., *Thin Solid Films*, **516** (2008) 5800.
- [25] EMERY N., WILDMAN E. J., SKAKLE J. M. S., MCLAUGHLIN A. C., SMITH R. I. AND FITCH A. N., *Phys. Rev. B*, **83** (2011) 144429.